JOURNAL OF APPLIED ELECTROCHEMISTRY 21 (1991) 208–212

Double-channel electrodes: Homogeneous kinetics and collection efficiency measurements

A. C. FISHER, R. G. COMPTON

Physical Chemistry Laboratory, South Parks Road, Oxford OX1 3QZ, UK

Received 26 February 1990; 3 May 1990

The theory of collection-efficiency measurements (under steady-state conditions) at double-channel electrodes has been extended to include the effects of homogeneous kinetics. In particular first- and second-order decompositions of the species electrogenerated at the upstream electrode have been examined. These problems have been treated numerically using the backwards implicit finite difference method. This theory is readily generalized to allow for more complicated homogeneous chemical reactions.

1. Introduction

The double-channel electrode arrangement (Fig. 1), pioneered by Gerischer [1], is a valuable approach to the study of intermediates and products of electrode reactions. The basis of such investigations is as follows. A solution species, A, passes over the upstream generator electrode where it is oxidized (or reduced) to a species B, i.e.

$$A \pm ne^- \rightleftharpoons B$$

The species B is then transported to the downstream detector electrode where it is analysed amperometrically, generally via reduction (or oxidation) back to A. The experiment is quantitatively characterized by the so-called "collection efficiency", N, given by

$$N = I_{det}/I_{gen} \quad (1)$$

where I_{gen} and I_{det} are the currents at the generator and detector electrodes, respectively. In particular the collection efficiency is lowered with respect to its value when B is stable if B decays in the gap between the electrodes. We have explored elsewhere the consequences of heterogeneous reaction of B on the surface of the gap [2]; in this paper we develop a generally applicable theory for the case of homogeneous decay.

Early work on double channel electrodes by Matsuda *et al.* [3–5] relies on the use of the Leveque approximation [6] in which the parabolic Poiseuille flow within the channel is linearized near the cell walls. This restricts the application of the early theory to conditions and geometries such that

$$\frac{V_f b}{D d x_1} \gg 1 \quad (2)$$

where V_f is the volume flow rate, D is the diffusion coefficient of the species of interest and b, d and x_1 are defined in Fig. 1. This limitation reduces the sensitivity and range of application of double channel electrodes. Accordingly we developed a theory of double-channel electrodes embracing all practical flow rates and cell geometries [7]. This eliminated the necessity of adopting the Leveque approximation by utilizing a numerical method (the backward implicit finite difference method) which allowed the parabolic character of the flow to be retained. In this way collection efficiencies were calculated for kinetically stable species as a function of electrode potential for both reversible and irreversible electron transfers; good agreement with experiment was found. In this paper we extend these calculations to allow for homogeneous decay of B. Specifically first- and second-order decompositions are examined. It is shown that these are readily and simply generalised to allow for more complex mechanistic chemistry.

2. Theory

The steady-state mass transport equation governing the convective-diffusion of a kinetically stable species in a channel cell in [6, 8], using the coordinate system of fig. 1, is given by

$$D_A \frac{\partial^2[A]}{\partial y^2} - v_x \frac{\partial[A]}{\partial x} = 0 \quad (3)$$

where D_A is the diffusion coefficient, [A] is the concentration of A, and v_x the solution velocity in the x-direction:

$$v_x = \left(\frac{6V_f}{bd}\right)\left(\frac{y}{b}\right)\left(1 - \frac{y}{b}\right) \quad (4)$$

The range of validity of Equation 3 in respect of "edge

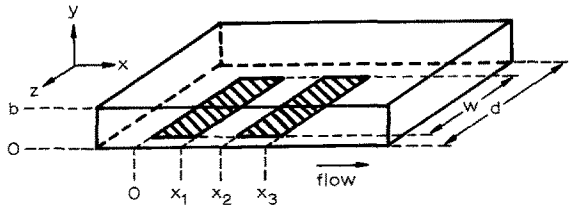

Fig. 1. The double-channel electrode geometry.

0021-891X/91 $03.00 + .12

effects" and other assumptions has been thoroughly examined [6, 8, 9].

In the double-electrode experiment outlined above, the product of the reaction at the upstream electrode, B, undergoes kinetic decay. Thus the transport equation for this species becomes

$$D_B \frac{\partial^2[B]}{\partial y^2} - v_x \frac{\partial[B]}{\partial x} - k_n[B]^n = 0 \quad (5)$$

for nth order kinetics. Equations 3 and 5 are soluble provided appropriate boundary conditions are specified. These are as follows:

Upstream of the generator electrode

$$x = 0; \quad [A] = [A]^*; \quad [B] = 0 \quad (6)$$

where [A]* is a bulk concentration.

At the generator electrode surface ($0 < x < x_1$; $y = 0$)

$$D_A \frac{\partial[A]}{\partial y} + D_B \frac{\partial[B]}{\partial y} = 0 \quad (7)$$

and

$$[A]/[B] = \exp(\theta) \quad (8)$$

where we have assumed a reversible redox process (standard electrode potential, E^0) and the normalized potential, $\theta = (F/RT)(E - E^0)$

At the surface of the 'gap' ($x_1 < x < x_2$; $y = 0$)

$$\frac{\partial[A]}{\partial y} = \frac{\partial[B]}{\partial y} = 0 \quad (9)$$

At the detector electrode ($x_2 < x < x_3$; $y = 0$)

$$[B] = 0 \quad (10)$$

where we have assumed the reduction (oxidation) of B back to A is transport-limited.

At the wall of the cell ($0 < x < x_3$; $y = b$)

$$\frac{\partial[A]}{\partial y} = \frac{\partial[B]}{\partial y} = 0 \quad (11)$$

The collection efficiency, N, is given by

$$N = \frac{I_{det}}{I_{gen}} = \left(D_B \int_{x_2}^{x_3} \left.\frac{\partial[B]}{\partial y}\right|_{y=0} dx\right) \Big/ \left(D_A \int_0^{x_1} \left.\frac{\partial[A]}{\partial y}\right|_{y=0} dx\right) \quad (12)$$

The convective-diffusion Equations 3 and 5 for A and B have been solved analytically by Matsuda [4] in the case of first-order kinetics only to yield collection efficiencies as a function of electrode geometry. As alluded to above, this approach involves the linearization of the velocity profile, v_x, viz

$$v_x \sim \left(\frac{6V_f}{bd}\right)\left(\frac{y}{b}\right) \quad (13)$$

This is the Leveque approximation [10] and, compared with Equation 4, it is clearly valid in the region $y \ll b$ or, equivalently, according to [6], where

$$Ddx_1 \ll V_f b \quad (14)$$

In order to produce results of a more general nature and, novelly, to permit the extension of the theory to second-order kinetics (and beyond to complex mechanisms), we have retained the full parabolic velocity profile, described by Equation 4, by using the backwards implicit finite difference method. We proceed as previously described in [7] using the same notation. The cell is divided into three regions ($0 < x < x_1$; $x_1 < x < x_2$; $x_2 < x < x_3$) and the backward implicit method is applied to each in turn. For each region, i($i = 1$, 2 or 3), the numerical solution involves covering the x–y plane with a finite difference grid of dimension $J \times K_i$. Values of J and K_i are chosen such that the solution converges to the required accuracy. In the calculations described $J = 500$, $K_i = 1000$ are satisfactory in the absence of kinetics: increasingly larger values are needed as k_n increases.

Increments are, in the x-direction, Δx, and in the y-direction Δy, where

$$y_j = j\Delta y \quad (j = 0, 1 \ldots J); \Delta y = b/J \quad (15)$$

$$x_k = k\Delta x \quad (k = 0, 1 \ldots K); \Delta x = x_i/K_i \quad (16)$$

x_i is x_1, $x_2 - x_1$ or $x_3 - x_2$ in the appropriate region. Derivatives are approximated to

$$\frac{\partial g^M}{\partial x} = \frac{g^M_{j,k+1} - g^M_{j,k}}{\Delta x}; \frac{\partial g^M}{\partial y} = \frac{g^M_{j+1,k+1} - g^M_{j,k+1}}{\Delta y} \quad (17)$$

$$\frac{\partial^2 g^M}{\partial y^2} = \frac{g^M_{j-1,k+1} - 2g^M_{j,k+1} + g^M_{j+1,k+1}}{(\Delta y)^2} \quad (18)$$

where g^M are normalized concentrations,

$$g^A = [A]/[A]^*; \; g^B = [B]/[A]^*. \quad (19)$$

We have previously shown [7] how this approach leads to a $(J-1) \times (J-1)$ matrix equation, for each of the species M = A or B, of the form

$$\begin{bmatrix} d_1 \\ d_2 \\ \cdot \\ \cdot \\ \cdot \\ d_j \\ \cdot \\ \cdot \\ \cdot \\ d_{J-2} \\ d_{J-1} \end{bmatrix} = \begin{bmatrix} b_1 & c_1 & 0 & & & & \\ a_2 & b_2 & c_2 & 0 & & & \\ \cdot & \cdot & \cdot & & & & \\ & \cdot & \cdot & \cdot & & & \\ & & \cdot & \cdot & \cdot & & \\ 0 & a_j & b_j & & c_j & 0 & \\ & & \cdot & & \cdot & & \cdot \\ & & & \cdot & & \cdot & \\ & & & & \cdot & & \cdot \\ & & & a_{J-2} & b_{J-2} & c_{J-2} & \\ & & & 0 & a_{J-1} & b_{J-1} & \end{bmatrix} \begin{bmatrix} u_1 \\ u_2 \\ \cdot \\ \cdot \\ \cdot \\ u_j \\ \cdot \\ \cdot \\ \cdot \\ u_{J-2} \\ u_{J-1} \end{bmatrix} \quad (20)$$

where the matrix elements are tabulated in the Appendix. The solution of the equations (in [7]) using an iterative procedure, also described previously in [11], yields the concentration profiles, $g^M_{j,k}$, over the whole x–y grid. The collection efficiency is then determined using Equation 12.

The computations were carried out via a FORTRAN 77 program executed on a VAX 11/785 mainframe computer, using NAG 11 library routines.

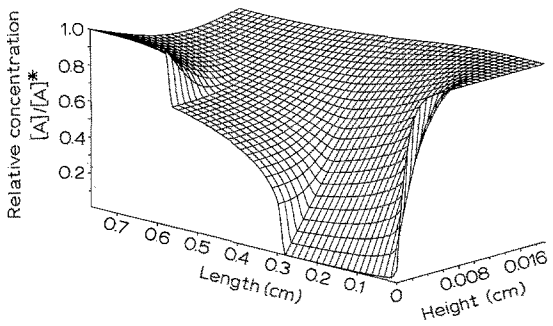

Fig. 2. The concentration profile of A within the channel flow cell for the no-kinetics case, calculated using the parameters: $b = 0.04\,\text{cm}$, $x_1 = 0.3\,\text{cm}$, $x_2 = 0.6\,\text{cm}$, $x_3 = 0.8\,\text{cm}$, $D = 7.6 \times 10^{-6}\,\text{cm}^2\,\text{s}^{-1}$. Note that the concentration profile is limited to the region $0 < y < b/2$.

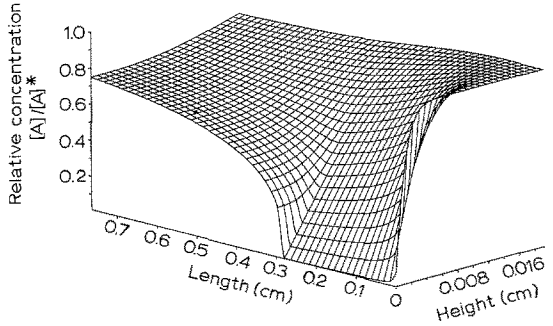

Fig. 4. The concentration profile of A within the channel flow cell for the first-order kinetics ($k_1 = 10.0\,\text{s}^{-1}$) case. The following parameters were used in the calculation: $b = 0.04\,\text{cm}$, $x_1 = 0.233\,\text{cm}$, $x_2 = 0.313\,\text{cm}$, $x_3 = 0.768\,\text{cm}$, $D = 7.6 \times 10^{-6}\,\text{cm}^2\,\text{s}^{-1}$. Note that the concentration profile is limited to the region $0 < y < b/2$.

3. Results and discussion

The numerical approach to the solution of the double-channel electrode convective-diffusion equations produced concentration profiles, $g^{\text{M}}_{j,k}$, as indicated above. Typical results can be seen in Figs 2 and 3 which were generated for the no-kinetics ($k_n = 0$) case. Figure 2 shows, as expected, that A is depleted in the vicinity of the generator electrode. This depletion is then partially relaxed in the zone of the gap by transport of A from bulk. Finally the detector electrode converts B back to A thus restoring the concentration of the latter to its bulk value at and near the surface of this electrode. Figure 3 shows the corresponding B profile. The introduction of kinetics produced analogous profiles: Figs 4 and 5 relate to the specific case of first-order kinetics ($k_1 = 10\,\text{s}^{-1}$) and were computed using the parameters specified in the figure legend. The loss of A, as compared to the no-kinetics case, through homogeneous decay is evident.

We consider next our results for first-order kinetics. Calculations were performed for a cell of geometry $x_1 = 0.233\,\text{cm}$, $x_2 = 0.313\,\text{cm}$, $x_3 = 0.768\,\text{cm}$, $b = 0.04\,\text{cm}$, $w = 0.6\,\text{cm}$ and $d = 0.4\,\text{cm}$ and for species with diffusion coefficients $D_A = D_B = 7.6 \times 10^{-6}\,\text{cm}^2\,\text{s}^{-1}$. The variation of I_{gen} and I_{det} as θ was varied through the reversible voltammetric wave on the generator electrode was examined. Figure 6 shows plots of I_{det} against I_{gen} for various rate constants, $k_1 = 0$, 0.001, 0.1, 0.5 and $1.0\,\text{s}^{-1}$. A linear relationship is, as expected, observed and the slopes of the lines correspond to the measured collection efficiency under these conditions.

Matsuda has calculated [4] the expected collection efficiency in the case of first-order kinetics under the assumption that the Leveque approximation is valid. With this assumption the collection efficiency is found to be a unique (geometry independent) function of the dimensionless rate constant,

$$\tilde{K}_n = \left(\frac{\tilde{k}_n}{D^{1/3}}\right)^{1/2}\left(\frac{b^2 dx_1}{3V_f}\right)^{1/3} \qquad (21)$$

where $\tilde{k}_n = k_n[\text{A}]^{*n-1}$, and simple approximate equations for the $N/\tilde{K}_1$ relationship result:

$$N/N_0 = \exp[-a'\tilde{K}_1^2 + b'\tilde{K}_1^4 - c'\tilde{K}_1^6] \qquad (22)$$

$$N/N_0 = \exp[-a'' + b''\tilde{K}_1^2 - c''\tilde{K}_1^4] \qquad (23)$$

where Equation 22 is valid for $0.08 < N/N_0 < 1$ and Equation 23 for $0.002 < N/N_0 < 0.1$. The coefficients a', b', c', a'', b'' and c'' depend upon electrode geometry and have been tabulated [4].

Figures 7 and 8 show how the collection efficiency varies with flow rate for the cell geometry specified above. Figure 7 relates to a first-order rate constant of $1\,\text{s}^{-1}$. Clearly as the flow rate is reduced more B is lost before it arrives at the detector electrode and thus the collection efficiency falls. Also shown in Fig. 7 is the

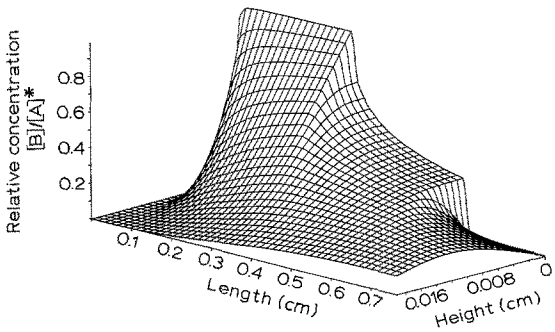

Fig. 3. The concentration profile of B within the channel flow cell for the no-kinetics case. Note that the concentration profile is limited to the region $0 < y < b/2$.

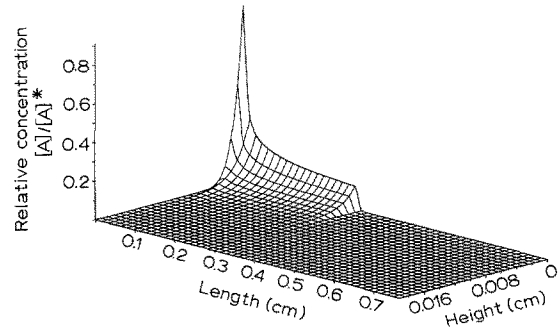

Fig. 5. The concentration profile of B within the channel flow cell for the first-order kinetics ($k_1 = 10.0\,\text{s}^{-1}$) case. The same parameters were used in the calculation as for Fig. 4. Note that the concentration profile is limited to the region $0 < y < b/2$.

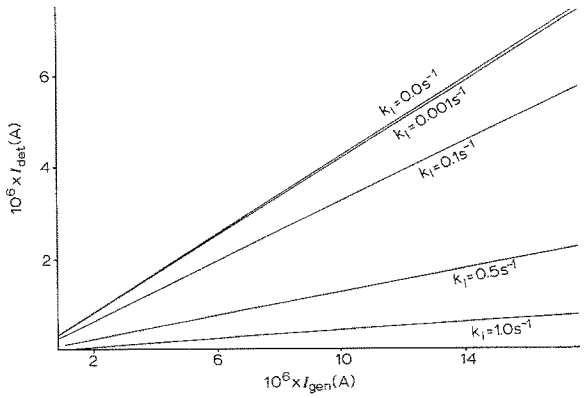

Fig. 6. Plots of I_{det} against I_{gen} for the case of first order kinetic decay of B, with $k_1 = 0.0, 0.001, 0.1, 0.5$ and $1.0\,s^{-1}$, calculated for the cell geometry specified in the text.

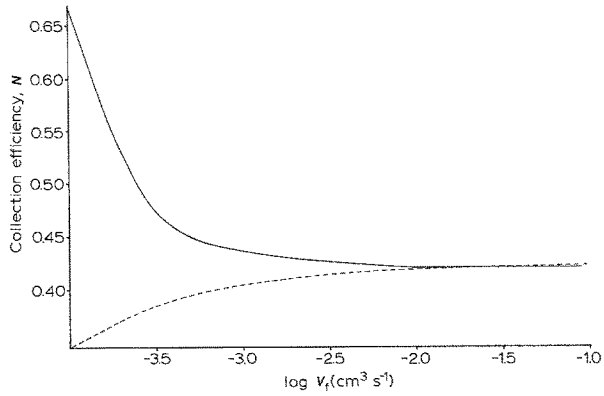

Fig. 8. The variation of the collection efficiency with the solution flow rate for the channel cell geometry specified in the text and $k_1 = 0.001\,s^{-1}$. The solid line shows the results of the backwards implicit calculations whereas the dotted line shows the approximate theory of Matsuda [4].

behaviour calculated according to Matsuda's approximate theory. It can be seen that in the limit of fast flow rates – where the Leveque approximation holds best – the two treatments agree. However, at lower flow rates the Matsuda treatment underestimates the collection efficiency. This error results from the fact that the Leveque approximation over estimates the solution velocity, v_x, away from the electrode. Thus the species B, under this approximation, is transported out of the cell before it can diffuse to the detector electrode. At higher flow rates, the diffusion layer is thin, the species B remains in the region $y \ll b$, and the two treatments converge. This effect is more dramatic in the case of slower kinetics. Figure 8 shows the equivalent plot to Fig. 7 but for a rate constant of $0.001\,s^{-1}$. Here the Matsuda theory predicts a slight decrease of N with decreasing flow rate. However, the convective behaviour described above is enough to induce the opposite trend and N actually increases as the flow drops – an effect we have previously seen in the case where B is stable (no-kinetics) [7]. The results under conditions where the Leveque approximation is valid can be summarized by fig. 9 which shows a 'working curve' relating N to $\tilde{K}_1$. This allows the analysis of all experimental data gathered under conditions where this approximation holds. Clearly from Figs 7 and 8, outside of these limits, experimental results must be analysed by the full computations outlined above.

We now turn to the consideration of the problem of the second-order decay of B of which we are unaware of any previous work. Figure 10 shows plots of I_{det} against I_{gen} for various rate constants, $k_2 = 0$, 10^5, 5×10^5, $5 \times 10^6\,mol^{-1}\,cm^3\,s^{-1}$ calculated using the same parameters as specified for the first-order case above. In this case a non-linear relationship is apparent: the higher the current density on the generator electrode the greater the effect of the homogeneous kinetics and, although N monotonically increases with I_{gen}, dI_{det}/dI_{gen}, steady falls. Clearly then N is a function of θ so that no universal working curve, even under Leveque conditions, can be given. However Fig. 11 shows the experimentally most convenient plot of N against $\tilde{K}_2$ for the particular case where the generator electrode is held a potential corresponding to the transport limited conversion of A to B under Leveque conditions for an electrode of the geometry specified for Fig. 10.

From the theory given above it is clear that the quantitative description of double-channel electrodes for the study of electrode reaction mechanisms can be readily achieved using the backwards implicit finite difference method. In particular the extension to com-

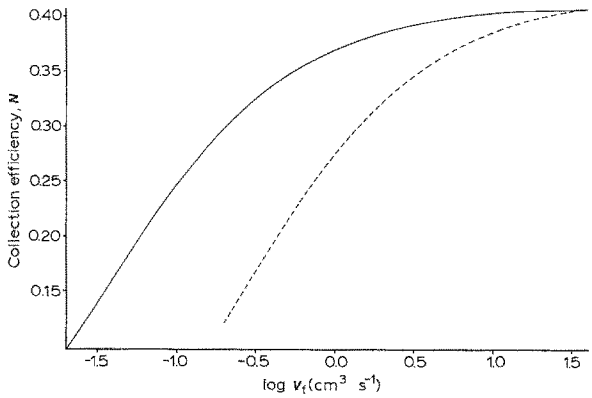

Fig. 7. The variation of the collection efficiency with the solution flow rate for the channel cell geometry specified in the text and $k_1 = 1.0\,s^{-1}$. The solid line shows the results of the backwards implicit calculations whereas the dotted line shows the approximate theory of Matsuda [4].

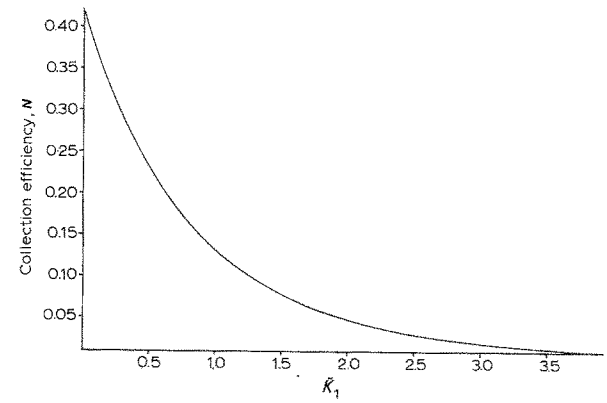

Fig. 9. A 'working curve' relating the collection efficiency to the normalized rate constant $\tilde{K}_1$ under conditions where the Leveque approximation holds.

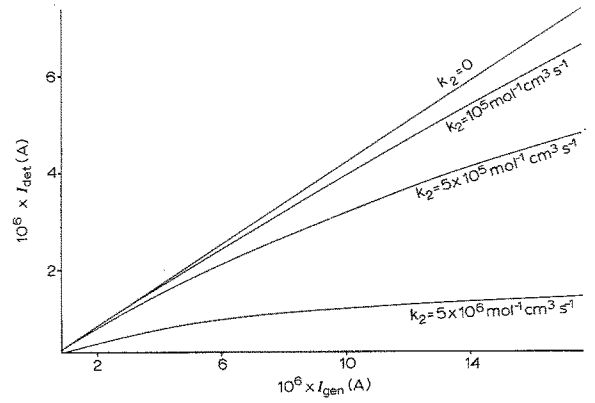

Fig. 10. Plots of I_{det} against I_{gen} for the case of second-order kinetic decay of B, with $k_2 = 0$, 10^5, 5×10^5, 5×10^6 mol^{-1} cm^3 s^{-1} calculated for the cell geometry specified in the text.

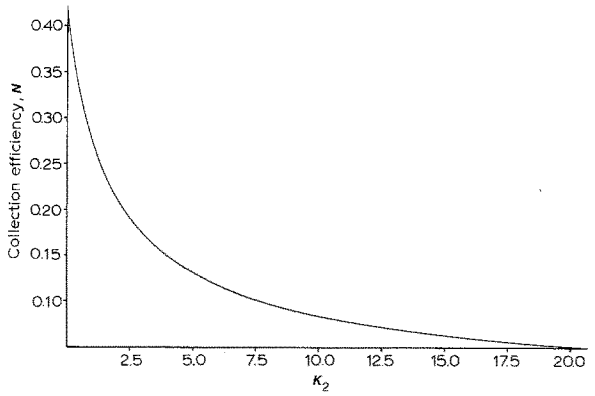

Fig. 11. A 'working curve' relating the collection efficiency to the normalized rate constant $\tilde{k}_2$ under conditions where the Leveque approximation holds and where the generator electrode is potentiostated at a value corresponding to the transport limited conversion of A to B.

plex electrode reaction mechanisms should present no conceptual or computational problem.

Acknowledgement

We thank SERC for the studentship awarded to ACF.

Appendix — The backward implicit method matrix equations

We have seen above that the application of the backward implicit method results in a $(J-1) \times (J-1)$ matrix equation of the form

$$\begin{bmatrix} d_1 \\ d_2 \\ \vdots \\ d_j \\ \vdots \\ d_{J-2} \\ d_{J-1} \end{bmatrix} = \begin{bmatrix} b_1 & c_1 & 0 & & & \\ a_2 & b_2 & c_2 & 0 & & \\ & \ddots & \ddots & \ddots & & \\ 0 & a_j & b_j & c_j & 0 & \\ & & \ddots & \ddots & \ddots & \\ & & & a_{J-2} & b_{J-2} & c_{J-2} \\ & & & 0 & a_{J-1} & b_{J-1} \end{bmatrix} \begin{bmatrix} u_1 \\ u_2 \\ \vdots \\ u_j \\ \vdots \\ u_{J-2} \\ u_{J-1} \end{bmatrix}$$

The various matrix elements now need to be specified. These are unchanged from those specified in [7], in respect of the corresponding 'no-kinetics' problem except as specified below:

Zone of the generator electrode $(0 < x < x_1)$

$$d_1^A = g_{1,k}^A + \frac{\lambda_1 g_{1,k+1}^B}{1 + \exp(-\theta)};$$

$$b_1^A = 1 + \lambda_1 \frac{(2 + \exp(\theta))}{(1 + \exp(\theta))};$$

$$d_1^B = g_{1,k}^B + \lambda_1 \frac{g_{1,k+1}^A}{(1 + \exp(\theta))} - (\tilde{k}*_1(\Delta y)^2 g_{1,k}^B/D);$$

$$b_1^B = 1 + \lambda_1 \frac{(1 + 2\exp(\theta))}{(1 + \exp(\theta))}$$

$$d_{j,k}^B = g_{j,k}^B - (\tilde{k}*_j(\Delta y)^2 g_{j,k}^B/D)$$

Zone of the gap $(x_1 < x < x_2)$

$$d_1^A = g_{1,k}^A;$$
$$d_j^A = g_{j,k}^A;$$
$$b_1^A = \lambda_1 + 1;$$
$$b_j^A = 2\lambda_j + 1;$$
$$d_1^B = g_{1,k}^B - (\tilde{k}*_1(\Delta y)^2 g_{1,k}^B/D);$$
$$b_1^B = \lambda_1 + 1;$$
$$d_j^B = g_{j,k}^B - (\tilde{k}*_j(\Delta y)^2 g_{j,k}^B/D);$$
$$b_j^B = 2\lambda_j + 1$$

Zone of the detector electrode $(x_2 < x < x_3)$

$$d_1^A = g_{1,k}^A + \lambda_1 g_{1,k+1}^B;$$
$$b_1^A = \lambda_1 + 1;$$
$$d_j^A = g_{j,k}^A;$$
$$b_j^A = 2\lambda_j + 1;$$
$$d_1^B = g_{1,k}^B - (\tilde{k}*_1(\Delta y)^2 g_{1,k}^B/D);$$
$$b_1^B = 2\lambda_1 + 1;$$
$$d_j^8 = g_{j,k}^B - (\tilde{k}*_j(\Delta y)^2 g_{j,k}^B/D);$$
$$b_j^B = 2\lambda_j + 1$$

where $\tilde{k} = k_n[A]*^{n-1}$.

References

[1] H. Gerischer, I. Mattes and R. Braun, *J. Electroanal. Chem.* **10** (1965) 553.
[2] R. G. Compton, G. M. Stearn, P. R. Unwin and A. J. Barwise, *J. Appl. Electrochem.* **18** (1988) 657.
[3] H. Matsuda, *J. Electroanal. Chem.* **16** (1968) 153.
[4] K. Aoki, K. Tokuda and H. Matsuda, *J. Electroanal. Chem.* **79** (1977 49.
[5] K. Aoki and H. Matsuda, *J. Electroanal. Chem.* **94** (1978) 157.
[6] P. R. Unwin and R. G. Compton, *J. Electroanal. Chem.* **205** (1986) 1.
[7] R. G. Compton and G. M. Stearn, *J. Chem. Soc., Faraday Trans. I*, **84** (1988) 4359.
[8] P. R. Unwin and R. G. Compton, *Comprehensive Chemical Kinetics* **29** (1989) 173.
[9] K. Aoki, K. Tokuda and H. Matsuda, *J. Electroanal. Chem.* **217** (1987) 33.
[10] M. A. Leveque, *Ann. Mines, Mem. Ser.*, **12/13**, (1928) 201.
[11] R. G. Compton, M. B. G. Pilkington and G. M. Stearn, *J. Chem. Soc., Faraday Trans. I*, **84**, (1988) 2155.